

# A Study of Composite Substrates for VHF and UHF Artificial Magnetic Conductors and Their Application to a SATCOM Antenna

Taulant Rexhepi<sup>1, \*</sup> and David Crouse<sup>2</sup>

**Abstract**—The bandwidth of Artificial Magnetic Conductor (AMC) structures based on the square patch geometry has been significantly increased by using composite ferrite particles. These magnetic composites are non-conducting materials which achieve extraordinarily high values of magnetic permeability in the VHF and UHF range. Two AMC designs are presented for two different bands: the lower VHF and the VHF/UHF bands. To realize the ultra-high bandwidth for those ranges two particular materials were considered; nickel zinc and bismuth strontium titanate based ferrites. The AMCs were designed and modeled via numerical simulations using real material parameters as reported in literature. A cross-dipole radiator was integrated with the AMC to create a wideband directive antenna for SATCOM applications.

## 1. INTRODUCTION

Ferrite materials have attracted antenna engineers for many years. Due to their high losses, they are commonly utilized as low-profile absorbers in anechoic chambers, as well being placed behind or around antennas to obtain directive radiation patterns, and good return loss characteristics [1].

For many applications antennas are required to be directional. To achieve this, absorbers are often used to eliminate the radiation in one direction so that the antenna only radiates in the opposite direction. In this arrangement, the absorbed radiation is converted into heat and otherwise wasted. In another, more useful configuration, a metallic groundplane is used to reflect the radiation in the desired direction. However, the key issue with using a metallic reflector is that the antenna cannot be placed very close to the metal reflector due to image currents traveling parallel to the antenna canceling out the fields and reducing radiation efficiency of the antenna. The ideal position to place the metal reflector is at quarter-wavelength distance from the radiating element, where the wavelength is that of the center operating frequency of the antenna system. This comes from the fact that the reflected radiation gains a propagation phase of  $180^\circ$  going to and coming from the groundplane which itself introduces a  $-180^\circ$  phase shift achieving a  $0^\circ$  reflection phase at the antenna plane. This is required for constructive interference which contributes to the gain increase. The antenna will operate efficiently as long as the reflected radiation does not destructively interfere with the radiation emitted in the forward direction. This occurs in the band where the phase of the reflected beam when measured at the surface of the antenna is between  $-90^\circ$  and  $90^\circ$ . For an antenna system using a classical air cavity between the radiator and the reflector at quarter wavelength away, the bandwidth of the system is one octave.

Directive antennas are used on air borne platforms for communications system such as satellite communications [2]. Planar antennas are often chosen because they allow operators to integrate the antenna system onto the body of the aircraft and use it as a groundplane. To ensure efficient operation of the aircraft the antenna system must conform as much as possible to the body of the aircraft. However

---

*Received 4 March 2016, Accepted 28 April 2016, Scheduled 6 May 2016*

\* Corresponding author: Taulant Rexhepi (trexhepi90@gmail.com).

<sup>1</sup> Electrical Engineering Department, The City University of New York, City College, 160 Convent Ave, New York, NY 10031, USA.

<sup>2</sup> Department of Electrical and Computer Engineering, Clarkson University, CU Box 5700, Potsdam, New York 13699, USA.

due to the low frequency the quarter wavelength distance is very large making the antenna system rather bulky. One approach to overcome this issue has been to place microwave absorbers between the radiator and groundplane allowing the antenna to operate efficiently while conforming to the aircraft. While effective, this technique is inefficient since the reflected radiation is not captured and wasted.

To overcome this physical constraint of the metallic reflector, metamaterials are used to create a low profile reflector in which the incident radiation is reflected without a phase [3]. The metamaterial is in the form of a planar metasurface consisting of square metal patches printed on a dielectric substrate. The metasurface is placed between the radiating element and the groundplane of the antenna. Together with the groundplane, the metasurface creates an Artificial Magnetic Conductor (AMC). AMCs induce capacitance and inductance to the electromagnetic radiation which cause a resonance from which the useful properties of the AMCs are drawn. Using these structures reduces the distance required between the radiating element and the antenna significantly.

The useful bandwidth of AMCs is dependent on the material properties of the underlying substrate namely that of magnetic permeability. Advances in material science, namely that of ferrite materials, has brought promise of further size decreases for antennas operating in the lower end of the RF spectrum. Ferrite materials significantly increase the useful bandwidth of the antenna system in consideration [4]. This paper serves the purpose of numerically investigating the potential and merit of using such materials for broadband AMCs and SATCOM antenna applications. The paper is organized as follows: in the subsequent section we introduce the design methodology for the square patch AMC, in Section 3 we introduce the two ferrite materials based on nickel zinc and bismuth strontium titanate to be used for AMCs in low VHF and VHF.UHF range respectively, we follow the section by introducing an integrated AMC with a VHF/UHF SATCOM antenna, and lastly provide a discussion of the numerical calculation results, and a conclusion.

## 2. METAMATERIAL SURFACE

Metamaterials are carefully designed composite structures which manipulate electromagnetic radiation in ways that materials existing in nature cannot. They can be designed for any part of the electromagnetic spectrum. These composites consist of periodic arrangements of unit cells which are designed to resonate at particular frequency where their useful properties are drawn. The dimensions of the unit cells of metamaterials are on the order of  $\lambda/10$ , where  $\lambda$  is the free space wavelength of the desired resonant frequency. This relation makes fabrication of metamaterials most efficient in RF domain since dimensions are fairly large and the structure can be made using.

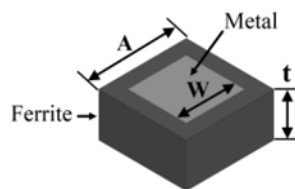


**Figure 1.** Unit cell based on the square patch geometry.

The AMC is a special type of metamaterial consisting of a top metasurface layer and the reflecting ground plane specifically designed for antenna applications. The planar metasurface consists of patterned unit cells which can be of various geometries. In this paper we will focus on the square patch geometry given in Fig. 1. Since the unit cells are small compared to the wavelength their electromagnetic properties can be expressed using lumped circuit elements [3]. The equivalent circuit model consist of a capacitor in parallel with an inductor. The lumped elements have resistors in series to account for losses. The value of the capacitance is directly related to the planar geometry of the unit cell and the dielectric properties of the underlying dielectric and can be found using [5]:

$$C = \frac{w}{\pi}(\epsilon_0 + \epsilon_1)\cosh^{-1}\left(\frac{a}{w-a}\right) \quad (1)$$

where,  $A$  is the length of the unit cell,  $w$  is the length of the metal patch,  $\varepsilon_0$  and  $\varepsilon_1$  are the permittivity values of free-space and the underlying dielectric respectively.

The inductance on the other hand only depends on only two parameters, one being the distance between the metasurface and the metallic ground plane  $t$ , and the other the permeability,  $\mu_r$ , of the medium between the two. The inductance is approximated by:

$$L = t\mu_r \quad (2)$$

However, one must note this equation is only valid for materials which do not exhibit a change of  $\mu$  with respect to frequency. Hence it is applicable to materials which do not exhibit a large  $\mu$  change. The circuit equivalence of the AMC allows one to analytically calculate the surface impedance of the AMC as a terminated parallel RLC transmission line. We know from basic circuit theory that inductance and capacitance contribute to the imaginary part of the impedance with a certain frequency dependence given by:  $X_L = j\omega L$ , and  $X_C = -j/\omega C$  where  $X_L$  and  $X_C$  are the impedance cause by an inductor and capacitance respectively. The total impedance of the system is given by:

$$Z = \frac{(R_L + X_L)(R_C + X_C)}{R_L + R_C + X_L + X_C} \quad (3)$$

where  $R_L$  and  $R_C$  are the series resistors of the inductor and capacitor, respectively. Resonance of the system occurs when  $X_L = X_C$  at frequency:

$$\omega = \frac{1}{\sqrt{LC}} \quad (4)$$

where,  $\omega_0 = 2\pi f_0$ . The reflection phase in the terminals of the circuit is analogous to the reflection phase of the AMC at the metasurface and is determined by:

$$\theta = \begin{cases} \pi - 2 \tan^{-1} \frac{X_i}{R_0}, & \text{if } X_i > 0 \\ -\pi - 2 \tan^{-1} \frac{X_i}{R_0}, & \text{if } X_i < 0 \end{cases} \quad (5)$$

From this relation we can see that the frequency at which the reflection phase 0 occurs when the impedance crosses infinity. Reflection phases of  $+90^\circ$  and  $-90^\circ$  occur when the  $X_i = R_0$  and  $-X_i = R_0$  respectively where  $R_0$  and  $X_i$  are the real and imaginary parts of  $Z$  respectively.

The relative bandwidth of the AMC can be approximated solely in terms of the AMC substrate and its magnetic parameter [6]:

$$B.W. \cong \frac{2\pi\mu_r t}{\lambda} \quad (6)$$

where  $\mu_r$ , and  $\lambda$  are the relative permeability of the substrate and wavelength of the desired resonance respectively. From Equation (6) one can see that the bandwidth is highly influenced by the permeability. Since it is desirable to keep the thickness of the antenna system as low as possible, in order to increase the bandwidth we consider an increased value of permeability. High values of  $\mu$  are very common for static magnetic fields and time varying fields with very small frequencies, however at RF frequencies materials that exhibit magnetic properties are non-existent in nature and must be artificially synthesized. This possibility of miniaturizing antennas has attracted many in material science field to develop such materials.

### 3. HIGH-PERMEABILITY MATERIALS

As previously shown, the inductance and capacitance of the AMC structure depend on the permeability and permittivity of the substrate respectively. Hence using a substrate which has a high permeability to permittivity ratio can significant increase the operational bandwidth of the AMC [7]. One such composite material which has such characteristics in the VHF range is the  $\text{Ni}_{0.8}\text{Cu}_{0.1}\text{Zn}_{0.05}\text{Co}_{0.05}\text{Fe}_{1.92}\text{O}_4$  ferrite [8]. At 30 MHz the permeability of the material peaks at around 108 while the epsilon has a value of only 15. The fabrication of these composite materials is detailed in [8]. The exact values

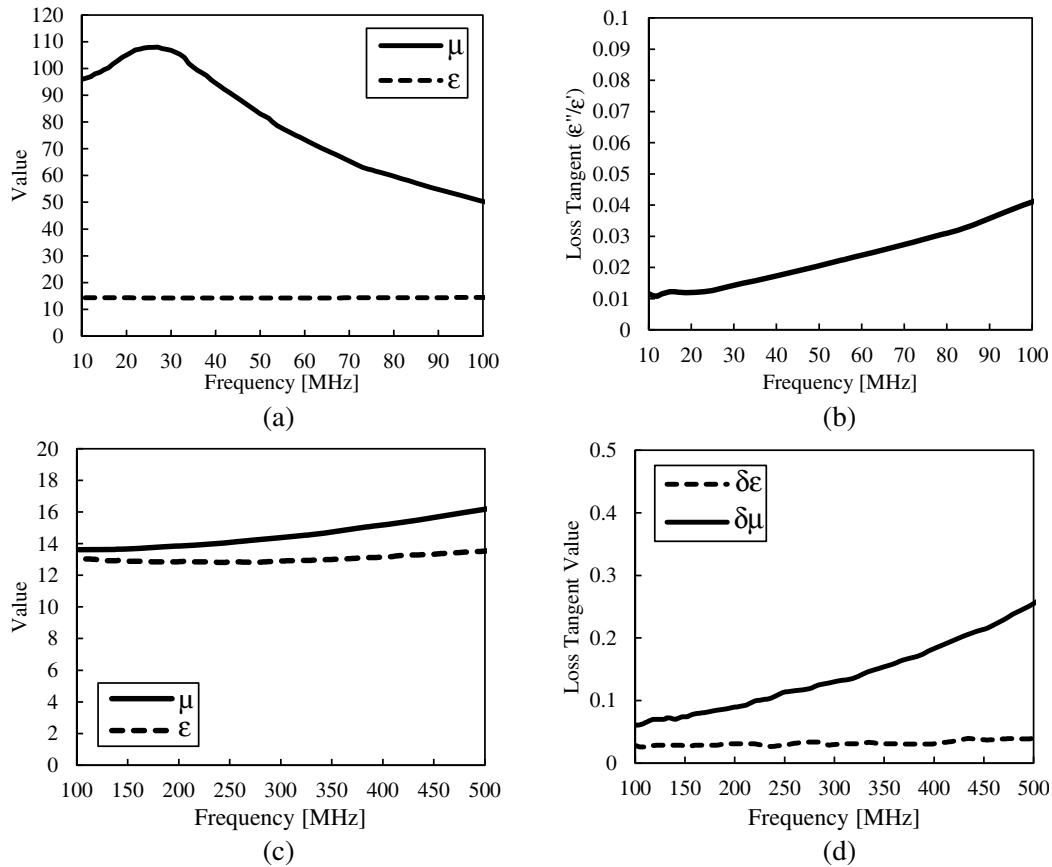


**Figure 2.** (a) Permeability and permittivity values; (b) and dielectric loss tangent for the  $\text{Ni}_{0.8}\text{Cu}_{0.1}\text{Zn}_{0.05}\text{Co}_{0.05}\text{Fe}_{1.92}\text{O}_4$  in the VHF range. (c) Permeability and permittivity values; (d) and dielectric loss tangent ( $(\text{Ba}_{0.5}\text{Sr}_{0.5})_3\text{Co}_2\text{Fe}_{24}\text{O}_{41} + 0.2\text{wt.}\% \text{WO}_3$ ) in the VHF/UHF range. All parameters were extracted from the results presented in [8].

for the material parameters are given in Fig. 3. Using these values we designed model a AMC for the VHF band using the square patch as the geometry Fig. 2 with a patch length of 52 mm and spacing of 15 mm between patches. The design comprised of three layers, the top layer consists of the printed metal patterns on a very thin layer (0.127 mm) of low-loss commercially available dielectric ( $\epsilon_r = 2.08$ ), this layer is mainly used as a buffer layer between the copper and the ferrite substrate and can be disregarded in the calculations for the equivalent capacitance. The following layer consists of the  $\text{Ni}_{0.8}\text{Cu}_{0.1}\text{Zn}_{0.05}\text{Co}_{0.05}\text{Fe}_{1.92}\text{O}_4$  ferrite with a thickness of 35 mm, followed by the metallic reflector. All of the metal in the design is half ounce copper. The overall thickness of the antenna system, considering a 1 mm thick planar antenna, is  $\lambda/200$  at the frequency where phaseless reflection occurs. This corresponds to a fifty fold decrease to the traditional quarter wavelength requirement.

The other material considered was also reported on by the same group and consisted of  $(\text{Ba}_{0.5}\text{Sr}_{0.5})_3\text{Co}_2\text{Fe}_{24}\text{O}_{41} + 0.2\text{wt.}\% \text{WO}_3$ . One very attractive feature of this particular material is that they are relatively low-loss [9]. This ensures that as much of the radiation as possible is reflected from the AMC and in the direction of the antenna. The frequency dependent values of the permeability, permittivity, and respective loss tangents have been extracted from the manuscript [8] and plotted in Fig. 2. The plots show that there is little change in the material properties around the VHF/UHF boarder making it ideal for antenna operating in that range. Using the reported material properties an AMC was designed with the center band at 300 MHz. Similarly, the square patch was used as the unit cell. The width of the patches are 23 mm with spacing between them of 15 mm. To obtain around one octave, typical of antennas operating in this range, the thickness of the ferrite substrate is 14 mm.

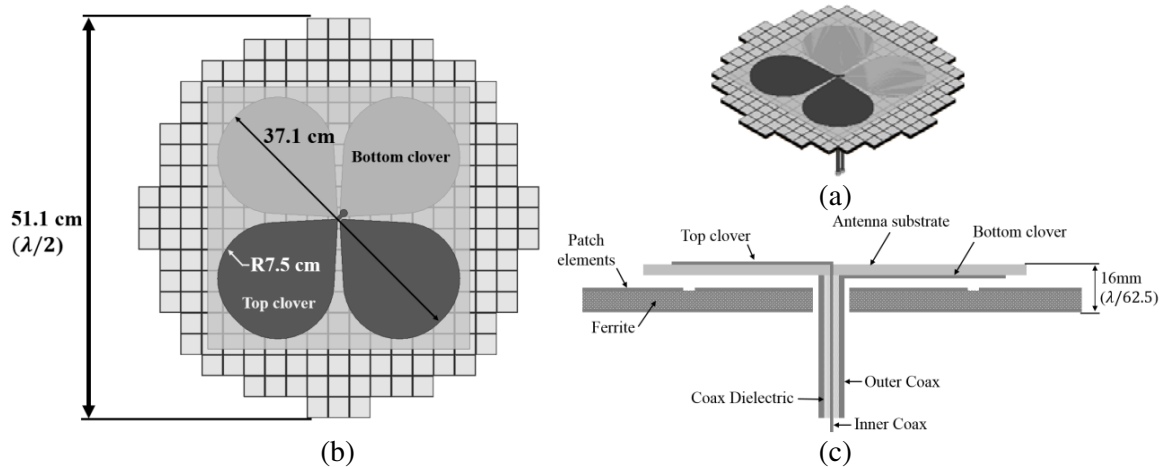


**Figure 3.** (a) Perspective view of antenna system; (b) top view of the antenna system with critical dimensions. (c) Side-view showing the feeding mechanism used to excite the radiator. Standard 50-ohm coax are used for the feed without a balun. Note that only one set of poles is shown here, similar scheme is used for the orthogonal poles as well.

#### 4. ANTENNA SYSTEM

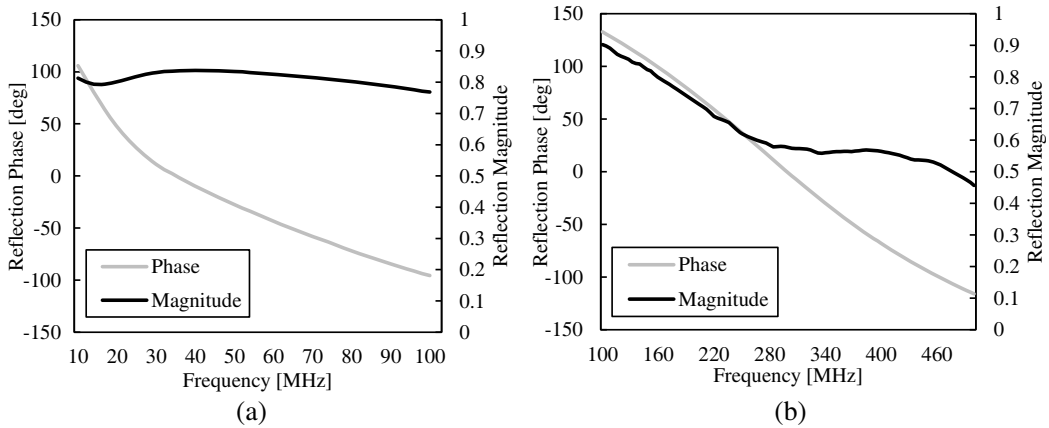
An antenna system based on planar cross-dipole radiator and AMC is designed for the VHF/UHF to verify the usefulness of the proposed AMC structure and analyze effects of the structures on common antenna parameters. The geometry of the radiator was based on the four-clover cross-dipole design which allows for slightly shortened length and relatively high gain [10]. This antenna is ideal for SATCOM applications particularly in airborne platforms. The very thin profile allows for the antenna to be easily integrated onto the fuselage or the wing of aircraft. The orthogonal poles are fed with two coaxial cables which attain a  $90^\circ$  phase shift between them to provide the necessary RHCP. To ensure efficient feeding system two of the clovers are located on top of the substrate meanwhile the other two are on the bottom. The substrate is based on the Neltec NY9220 dielectric ( $Dk = 2.2$ ) with a thickness of 1.2 mm. The jacket of the coax is connected to the bottom part while the inner coax goes through the antenna substrate to the top clover [11], this is illustrated in Fig. 3(c). The frequency of operation of the proposed antenna system is 240–380 MHz covering the Multiple User Objective System (MUOS) frequency bands as well as earlier Department of Defense legacy bands [12]. Dimensions and geometry of the radiator are given in Fig. 3(a). Small dimensions of the AMC unit cell allow for the geometry of the reflector to be made in a circular form such that the radiation pattern is the maintained for different phi angles. Square patches comprise the unit cells of the AMC used in the antenna simulation with the following dimensions:  $A = 30$  mm,  $W = 28$  mm, and  $t = 9$  mm. The substrate was based on the  $(\text{Ba}_{0.5}\text{Sr}_{0.5})_3\text{Co}_2\text{Fe}_{24}\text{O}_{41} + 0.2\text{wt.}\% \text{WO}_3$  ferrite previously discussed.

#### 5. DISCUSSION

Reflection phases of the AMCs were numerically calculated using ANSYS HFSS software, from which the bandwidth was also determined as well as reflection magnitude. The material properties used in the simulations attained frequency dependent values as reported in the plots in Fig. 2. Both real and imaginary values of the relative values of the relative permittivity and permeability were used where available. For the  $\text{Ni}_{0.8}\text{Cu}_{0.1}\text{Zn}_{0.05}\text{Co}_{0.05}\text{Fe}_{1.92}\text{O}_4$  material only the dielectric loss tangent was available, hence to obtain more realistic results a constant magnetic loss tangent of 0.1 was used which is twice as much as the highest dielectric loss tangent observed for the material. A summary of results is presented in Table 1. We will identify AMC 1 and AMC 2 as the lower VHF and VHF/UHF AMCs respectively. In the case of the AMC 1 the frequency in which the reflection phase crosses zero is not occur at the center of the operating band. Which resulted from the fact that the permeability of the substrate highly varies

**Table 1.** Summary of Results.

Parameter	AMC 1	AMC 2	SATCOM Antenna System & AMC
Resonant Frequency	35 MHz	300 MHz	300 MHz
Bandwidth	154%	88%	50%
Range of Operation	13–94 MHz	175–440 MHz	240–380 MHz
Thickness ( $t$ )	35 mm	14 mm	9 mm
Unit-cell length ( $A$ )	67 mm	38 mm	30 mm
Metal patch length ( $W$ )	52 mm	23 mm	28 mm
Antenna RHCP Gain	-	-	$\sim 3.2$ dB
Axial ratio ( $-/+60^\circ$ )	-	-	$< 3$ dB

**Figure 4.** Reflection phase shift and magnitude for (a) AMC 1 and (b) AMC 2.

with frequency. The bandwidth as previously defined is roughly five octaves from 20 MHz (Fig. 4(a)) making ideal for HF radio communication and Single Channel Ground and Airborne Radio Systems (SINCGARS) antennas. For most of the useful frequency band, the reflection phase is below zero which can be offset by the propagation phase to and from the AMC. The reflector can also be designed to have a phase gradient which can be used to create an ultra-thin focusing reflect-array for astronomical radio astronomy. The reflection magnitude was based solely on the dielectric loss-tangent since only that was available (Fig. 4(a)) AMC 2 also achieves a very wide band response with an extraordinarily thin profile. The bandwidth for this system was one octave ranging from 200–400 MHz. Fluctuations of the permeability with respect to frequency were minimal hence the reflection phase represents the S-type response which one accustomed to seeing (Fig. 4.) All losses were taken into account in this analysis, the reflection magnitude shown in Fig. 4(a) varies highly with frequency.

The reflection magnitude averages out to around 60% of the incident radiation in which case the gain of the antenna in the forward direction would be improved by approximately 2–4 dB. AMC 1 and 2 were designed using plane-wave excitation, however the radiation emitted from the cross-dipole radiating element cannot be approximated by a plane wave in the near-field where the AMC is located. To account for this the AMC used in the antenna simulations had slightly varied dimensions which were optimized to couple with the SATCOM cross-dipole radiating element.

The antenna system introduced in Section 4 was simulated and various antenna parameters were numerically calculated. The antenna overall thickness is only 16 mm making it very low-profile. Return loss of the antenna shows that the antenna achieves a fairly wide bandwidth covering a significant part of VHF/UHF SATCOM bands (Fig. 5(a)). The gain of the antenna achieves a peak value of 4 dB at 380 MHz and an average value of around 4 dB for the operational band. The radiation pattern is

maintained through the operational bandwidth of the antenna, due to the carefully designed ground plane very little variation occurs for different values of  $\phi$ . Fig. 6 shows the radiation pattern for different frequencies at three  $\phi$  values. Slight variation of the pattern is observed, a result of the asymmetrical feed. Axial ratio showing the ratio of the orthogonal polarizations is an important parameter for circularly polarized antennas and particularly important in cases where antennas are atop aircraft. The antenna must maintain good circular polarization as the aircraft banks to different angles. The boresight axial ratio for the antenna is maintained than 3 dB for the operational band

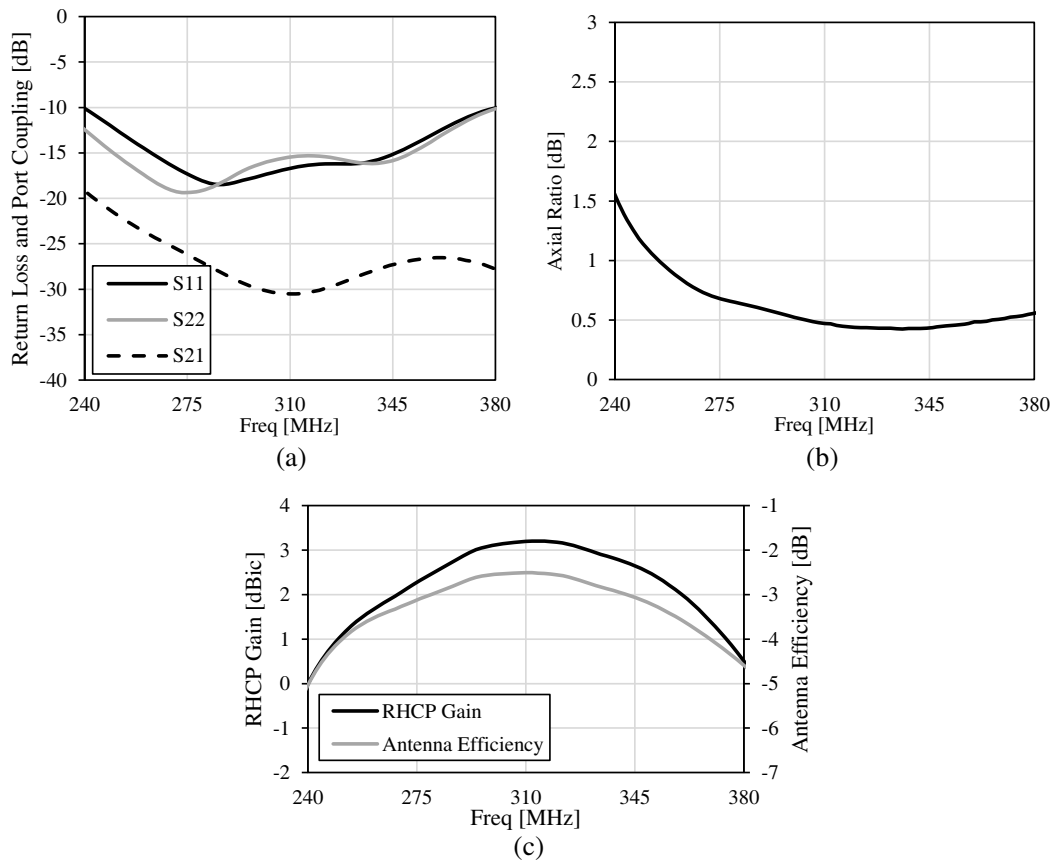


**Figure 5.** (a) Return loss and port coupling, simulated boresight axial ratio (b), and simulated RHCP gain at boresight and antenna efficiency (c) of antenna system discussed in Section 4.

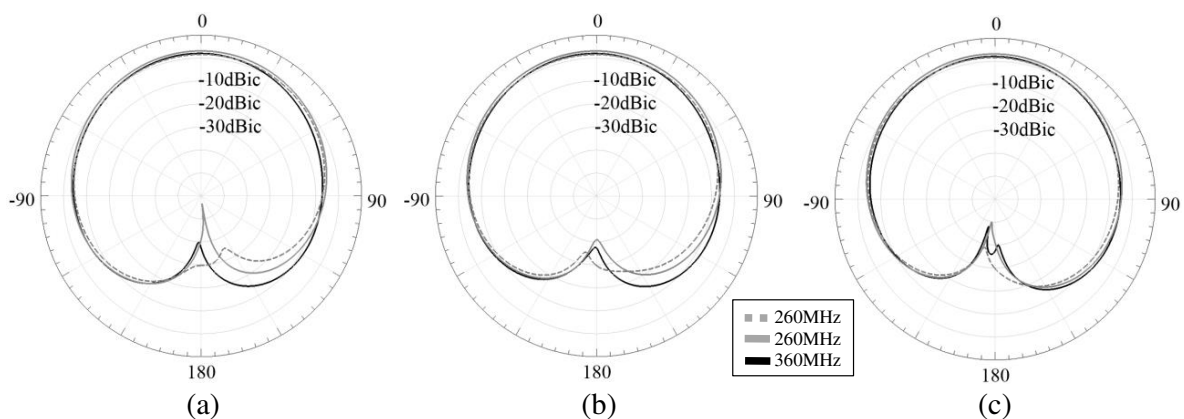


**Figure 6.** Simulated radiation patterns of the RHCP gain for the above frequencies at (a)  $\phi = 0^\circ$ , (b)  $\phi = 45^\circ$ , and (c)  $\phi = 90^\circ$ , legend of frequencies shown below applies to all plots.

(Fig. 5(c)).

One of the drawbacks for using ferrites in miniaturizing antenna systems is the fact that they are quiet lossy and poses high weight characteristics. The lossy characteristics are evident in the antenna efficiency plot as the antenna only achieves a  $-2$  dB peak efficiency (Fig. 5(b)). Likewise for the weight, such ferrites are heavily based on iron composites which are densely packed molecules leading to increased weight. Depending on processing technique [13] the density of the ferrites ( $\text{Ba}_{0.5}\text{Sr}_{0.5}\text{Co}_2\text{Fe}_{24}\text{O}_{41}$ ) used in the antenna structure are roughly  $4.75 \text{ g/cm}^3$ . Which translates to an estimated weight of 10 kg for the antenna system. Hence the significant size decrease comes at the expense of the antenna system weight increase.

## 6. CONCLUSION

Ultra-wide band AMCs were designed and modeled for antenna applications in two separate RF regimes. The AMCs were based on the simple square patch geometry which would significantly reduce manufacturing costs. High permeability materials based on nickel-zinc ferrites and bismuth strontium titanate were used as the AMC substrates. Two variations were modeled, one designed to operate in the lower VHF band, and the other in the VHF/UHF border. The high permeability to permittivity ratio of the  $\text{Ni}_{0.8}\text{Cu}_{0.1}\text{Zn}_{0.05}\text{Co}_{0.05}\text{Fe}_{1.92}\text{O}_4$  ferrite allows for an exceptional bandwidth performance with a very low profile for planar antennas in the 13–94 MHz range. A cross-dipole radiator was integrated with an AMC which created a very low-profile antenna system. It was shown that important antenna parameters are maintained while achieving a significant size decrease.

## ACKNOWLEDGMENT

This work was supported by the NSF Industry/University Cooperative Research Center for Metamaterials (grant number IIP-1068028).

## REFERENCES

1. Kern, D. J. and D. H. Werner, “Magnetic loading of EBG AMC ground planes and ultrathin absorbers for improved bandwidth performance and reduced size,” *Microwave and Optical Technology Letters*, Vol. 48, No. 12, 2468–2471, 2006.
2. Zhou, H., M. Jong, and G. Lo, “Evolution of satellite communication antennas on mobile ground terminals,” *International Journal of Antennas and Propagation*, 2015.
3. Sievenpiper, D., et al., “High-impedance electromagnetic surfaces with a forbidden frequency band,” *IEEE Trans. Microwave Theory and Tech.*, Vol. 47, No. 11, 2059–2074, 1999.
4. Diaz, R., “Magnetic loading of artificial magnetic conductors for bandwidth enhancement,” *IEEE Antennas and Propagation Society International Symposium*, Vol. 2, 2003.
5. Suraperwata, A. V., L. Olivia, and A. Munir, “Inductance and capacitance reformulation of square patch-based artificial magnetic conductor,” *Proc. 7th International Conference on Telecommunication Systems, Services, and Applications (TSSA)*, 187–191, 2012.
6. Diaz, R. E. and S. A. Clavijo, “Artificial magnetic conductor,” *Encyclopedia of RF and Microwave Engineering*, 2005.
7. Rexhepi, T. and D. Crouse, “Ultra-wide band metasurface for low-profile RF antenna applications based on high-Mu low-epsilon composites,” *Proc. 6th International Conference on Metamaterials, Photonic Crystals and Plasmonics, META’15*, 596, 2015.
8. Su, H., et al., “Low-loss magneto-dielectric materials: Approaches and developments,” *Journal of Electronic Materials*, Vol. 43, No. 2, 299–307, 2014.
9. Petrov, R. V., et al., “Antenna miniaturization with ferrite ferroelectric composites,” *Microwave and Optical Technology Letters*, Vol. 50, No. 12, 3154–3157, 2008.
10. Rexhepi, T., et al., “Low profile UHF/VHF metamaterial backed circularly polarized antenna structure,” *Progress In Electromagnetics Research C*, Vol. 60, 11–20, 2015.

11. Zimmerman, M. L., I. E. Timofeev, and L. Wu, "Tri-pole antenna element and antenna array," *U.S. Patent*, No. 9, 077,070, 2015.
12. Oetting, J. D. and T. Jen, "The mobile user objective system," *Johns Hopkins Apl. Technical Digest*, Vol. 30, No. 2, 103–112, 2011.
13. Hill, M. D., "Specialty materials processing techniques for enhanced resonant frequency hexaferrite materials for antenna applications and other electronic devices," *U.S. Patent*, No. 8, 609,062, 2013.